Atomic-structure characterization of a H:GaAs(110) surface by time-of-flight ion-scattering spectrometry

J. E. Gayone, R. G. Pregliasco, E. A. Sánchez, and O. Grizzi

Centro Atómico, Bariloche and Instituto Balseiro, Comisión Nacional de Emergia Atómica and Consejo Nacional de Investigacions Cientificas y Técnicas, 8400 San Carlos de Bariloche, Río Negro, Argentina

(Received 3 December 1996)

We have used ion-scattering spectrometry with time-of-flight analysis (TOF) to study the atomic structure of a GaAs(110) surface exposed to atomic hydrogen. The TOF spectra of ions plus neutrals acquired for 6 keV Ne^+ backscattering from both As and Ga top-layer atoms show a strong dependence on the projectile incidence direction and on the hydrogen exposure. The variations in the quasisingle backscattered intensity derived from the TOF spectra were analyzed with a code that calculates shadowing and focusing regions in a two-atom model. Measurements as a function of the hydrogen exposure indicate that the surface derelaxes approaching the ideal bulk termination. At the beginning of the adsorption the fraction of the surface that undergoes derelaxation increases very fast with exposure. At higher exposures, the rate of derelaxation becomes slower and the TOF spectra tend to a steady state. From Ne quasisingle backscattered intensities, measured as a function of the incident angle, we have determined that the spacing between the top As and Ga layers is reduced from ($\Delta Z = 0.66 \pm 0.08$) Å for the clean surface to ($\Delta Z = 0.0 \pm 0.08$) Å for intermediate exposures (2000 L H_2). At this exposure we have found a spacing between the first and second layers of (1.8 ± 0.1) Å. At higher exposures the results indicate a small counter-relaxation. [S0163-1829(97)06828-8]

I. INTRODUCTION

Hydrogen atoms can saturate the dangling bonds of semiconductor surfaces and modify both their electronic properties and the atomic structure of the topmost surface layers. Although hydrogen might be considered as the simplest adsorbate, its interaction with semiconductor surfaces still presents unsolved aspects. To some extent this is due to the fact that only a few surface analysis techniques are sensitive to hydrogen. In the case of hydrogen chemisorption on GaAs(110) an additional difficulty arises from the fact that molecular hydrogen does not adsorb on the surface. The exposures require dissociation of H_2 by means of a hot filament, making uncertain the comparison of coverages used in different laboratories.

The generally accepted atomic structure of the clean GaAs(110) surface is shown schematically in Fig. 1(a). The surface buckling angle ω characterizing the relaxation, defined by the angle of rotation of consecutive As and Ga rows [Fig. 1(a)], has been measured by several techniques[1–5] and calculated using different approximations.[6,7] The values obtained span over the range of $\omega = 25°$ to $\omega = 31°$.

Every surface analysis technique applied to the H:GaAs(110) surface has provided a piece of information about this system. Based on experiments of high-resolution electron energy-loss spectroscopy (HREELS), Lüth and Matz[8] and del Pennino et al.[9] have shown that even for very low adsorption doses, H chemisorbs on both Ga and As surface atoms. From EELS measurements it has been proposed[10] that the observed quenching of the $3d$ Ga exciton transition corresponds to a monolayer (ML) coverage. However, there are measurements suggesting that the surface may reach a steady regime with some of the dangling bonds not saturated. For example, in a high-resolution photoemission

study,[11] the clean surface components in the As and Ga core level signals were not completely quenched, and in an angle-resolved photoemission study[12] some traces of the clean surface states were present, together with the persistence of the Ga $3d$ exciton, even for high exposures. A study as a function of the H_2 dose, involving Auger electron spectroscopy, EELS, low-energy electron diffraction (LEED) and photoemission yield spectroscopy,[13] has shown that H interacts with the surface in a two-step process: first, an adsorption stage which saturates with one H per surface atom, and then a dissociation stage with the surface forming a rough Ga-rich substrate with a hydrogenated species of As.

Calculations based on the functional density formalism indicate that full and half monolayers of H atoms change the relaxation of the whole surface;[16–18] the Ga atoms move to positions sligtly above the As atoms giving rise to a small counter-relaxation ($\omega < 0°$). More recent calculations for a coverage of 1/4 ML (Ref. 19) have predicted that derelaxation occurs only for those surface atoms that are bound to H atoms, with a resulting buckling angle $\omega = 6°$. Contrary to the case of the clean surface, there are few experimental determinations of the atomic structure of the H:GaAs(110) surface. From the attenuation of the LEED spots and the photoemission yields measured as a function of the H exposure, M'Hamedi et al.[13] concluded that the adsorbed H atoms derelax the surface (in this work, no quantitative determination of the surface atomic position was performed). More recently, using grazing incidence x-ray diffraction[14] (GIXD) and photoelectron diffraction (PD),[15] Ruocco et al., assuming H coverages of 1 and 1/4 ML, have proposed values for ω of $-5°$ and $6°$, respectively.

In the present work we use ion-scattering spectrometry combined with time-of-flight analysis (TOF-ISS) to study the H:GaAs(110) surface for different H exposures. The aim of
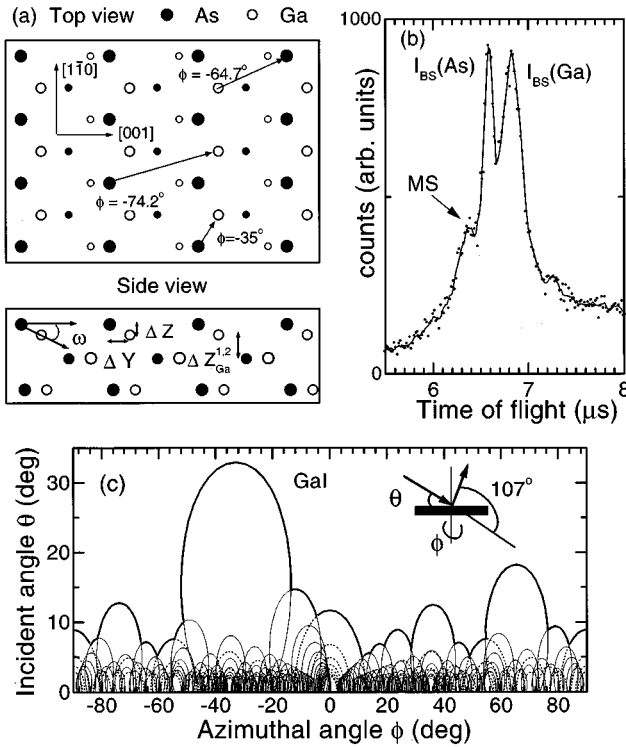
FIG. 1. (a) Top and side view of the clean GaAs(110) surface. The azimuthal angle ϕ is measured from the $[1\bar{1}0]$ direction, with negative values for clockwise rotation. The buckling angle ω and characteristic interlayer spacings are shown in the side view. (b) TOF spectra of ions plus neutrals measured at $(\phi,\theta)=(-64.7°,8.3°)$ for 6 keV Ne$^+$ scattering from the clean surface. (c) Shadowing regions for 6 keV Ne$^+$ scattering from first layer Ga atoms displayed in the incident and azimuthal angles, as defined in the inset. Regions inside the thin solid lines correspond to shadowing by As top layer atoms, those within the dotted lines are due to other Ga atoms located in the same layer. The thick line indicates the focusing condition.

the work is to determine the atomic structure of the derelaxed fraction of the surface and to obtain information about the dependence of the derelaxation process on the H$_2$ exposure.

We have shown in a previous work[5] (here referenced as paper I) that the TOF-ISS technique is a very sensitive tool in determining the position of the atoms in the first layer and that it can reproduce the accepted value for the relaxation of the clean GaAs(110) surface with great accuracy. Since the hydrogen layer produces a small effect on keV heavy-ion trajectories, TOF-ISS should be able to detect the changes in the surface atomic structure with an accuracy similar to that of the clean surface. A difference between TOF-ISS and the diffraction techniques used to study this surface[13–15] is that it samples directly (in real space) the ion core positions and that along certain crystallographic directions it is relatively easy to separate the contributions of the top layer from those of deeper layers. To our knowledge this is the first time that ion-scattering spectrometry is applied to the study of the H:GaAs(110) surface.

The work is organized as follows: in Sec. II we briefly describe the experimental details together with the code used to analyze the data, and in Sec. III the experimental results

are presented and compared with shadowing and focusing regions calculated with the code. This section is divided into four parts: first, TOF spectra are discussed for different H exposures; then we discuss the effect that the adsorbed H may have on the projectile trajectories; after this we present the variations of the projectile backscattered intensities with (a) the incidence direction at a fixed H exposure and (b) with the exposure at fixed incidence. Finally, a comparison with results obtained in other laboratories and the conclusions are summarized in Sec. IV.

II. EXPERIMENTAL METHOD

The surface of a zinc-doped GaAs(110) crystal was prepared by cycles of grazing bombardment with 20 keV Ar$^+$ at 1.5° incidence and annealing at 500 °C. We have shown in paper I that this method is efficient to clean the surface and to smooth out small surface imperfections. For a detailed description of the beam-pulsing optics, detection system, sample cleaning, and orientation inside the UHV chamber, we refer to paper I. Before taking the TOF-ISS spectra, the cleaning cycles were performed for about 2 h to smooth out defects produced in previous measurements. No traces of C and O were detected by Auger electron spectroscopy after this treatment. Atomic H was obtained by dissociation of high purity molecular hydrogen with a hot W filament placed at 6 cm from the surface. As the dissociation rate strongly depends on the size and temperature of the filament, as well as on the distance to the surface, it is difficult to relate the molecular exposure given here with fractions of ML or with experiments done at other laboratories. For this reason, following previous works[8–15] the exposures are given in Langmuirs of H$_2$ (1L$=10^{-6}$ Torr sec).

All the spectra shown in this work have been recorded with 6 keV Ne$^+$ projectiles. The TOF analysis was performed at a fixed scattering angle of 107°, with a flight path of 110.5 cm. Figure 1(b) shows a typical spectrum taken for the clean surface along the direction $(\phi,\theta)=(-64.7,8.3)$° [see the inset of Fig. 1(c) for the angle definition]. The peak at lower (higher) TOF corresponds to Ne ions plus neutrals scattered off As (Ga) target atoms in quasisingle collisions. The second peak is broader because both ^{69}Ga and ^{71}Ga isotopes contribute with similar abundance (40 and 60%, respectively). The shoulder at low time of flight is due to multiple-scattering (MS) events. This contribution usually appears strong at incident angles greater than those necessary to penetrate the first atomic layer (around 6° at this direction).

We have performed two kinds of measurements: (a) TOF spectra taken as a function of the incident angle for fixed azimuthal orientation and H$_2$ dose, and (b) TOF spectra taken along fixed incidence conditions as a function of the H$_2$ dose. The contributions to the backscattered intensity coming from quasisingle collisions with As or Ga atoms [I_{BS}(As) or I_{BS}(Ga)] show strong rises at specific (ϕ,θ) directions which are due to focusing of the ion trajectories by the atomic potentials. For $\theta<30°$ these critical angles are determined mainly by the relative position of the target atoms in the first two atomic layers (paper I); deeper layers contribute to the backscattering intensity through sequences of multiple collisions and therefore appear at somewhat dif-

ferent scattered energies (they contribute to the shoulder and broad background observed below the quasisingle peaks). The separation of these two contributions is described in paper I and in Sec. III C.

The information about the position of the surface atoms is obtained from the comparison of critical angles measured with shadowing regions calculated with the code described in paper I. Figure 1(c) shows an example of the shadowing regions calculated for the first layer of Ga atoms. For a specified surface atom and an assumed surface atomic structure, the code calculates the shadow cones using Oen's formula,[20] and displays them in the main angular parameters of the experiment, i.e., the incident and azimuthal angles. In the calculation of the shadow cones for the relaxed (clean) surface we have used the vertical displacement ΔZ determined in paper I, ΔY from Ref. 2 and the Thomas-Fermi-Molière interatomic potential with the Firsov screening length multiplied by 0.63. This value was obtained from calibration against known interatomic distances in the clean surface (paper I). The thin solid lines in Fig. 1(c) correspond to shadowing regions produced by neighboring As atoms while the dotted ones come from neighboring Ga atoms. For incidence directions that are well inside the shadowing region, i.e., below the thick line in Fig. 1(c), the projectile intensity backscattered from Ga atoms $I_{BS}(Ga)$ should be very low unless a large amount of defects are present in the surface. Close to the thick line, there is focusing of the incidence trajectories onto the Ga atoms and a sharp rise of $I_{BS}(Ga)$ should be expected; according to the calibration used in paper I the focusing line should correspond to 70% of the $I_{BS}(Ga)$ rise (all the critical angles discussed in this paper are also measured at 70% of the rise in the intensity). Finally, well above the focusing line, the Ga atoms are visible to the beam, the ion trajectories are not distorted by focusing effects, and the Ga layer should contribute to $I_{BS}(Ga)$ with almost no dependence on the incident angle. Using a mapping that will be described elsewhere,[21] the code also calculates the angular regions where the outgoing projectile trajectories are blocked. These blocking regions affect only the trajectories backscattered from the first and second layers at incident angles much larger than those used in the present work. At the incident angles used here the only outgoing trajectories that are blocked are those coming from the third and deeper layers.

III. EXPERIMENTAL RESULTS AND DISCUSSION

A. TOF spectra

Figure 2 shows two sets of TOF spectra for 6 keV Ne[+] scattering from the clean and the hydrogenated GaAs(110) surfaces. The spectra were taken at a fixed azimuthal angle $\phi = -64.7°$ and incident angles $\theta = 5.5°$ (a) and $\theta = 8.3°$ (b). To interpret the behavior of the spectra with the H$_2$ exposure we first refer to the shadowing diagrams corresponding to the clean (i.e., relaxed) surface shown in Fig. 3. It can be seen in this figure that at these particular incidence directions (indicated by crosses) the contributions to $I_{BS}(As)$ and $I_{BS}(Ga)$ come from the topmost As and Ga layers (AsI and GaI). Deeper layers are well inside the shadowing regions and cannot contribute to the quasisingle scattering peaks. At $\theta = 5.5°$ $I_{BS}(As)$ is large because the incident angle is slightly above

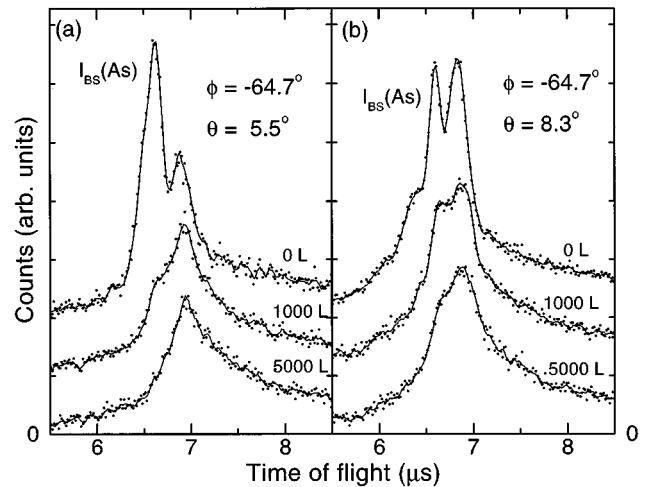the critical angle for focusing; at $\theta = 8.3°$ it decreases to a steady value and at the same time a shoulder at lower TOF (higher energy) due to multiple scattering starts to be seen. On the other hand, $I_{BS}(Ga)$ is low at $\theta = 5.5°$ (slightly below the focusing line) and becomes large at $\theta = 8.3°$ due to a focusing produced by an As atom.

The TOF-spectra change upon H$_2$ exposure, the main change being the strong attenuation of $I_{BS}(As)$, which almost disappears for an exposure of 5000 L (Fig. 2). At $\theta = 8.3°$ $I_{BS}(Ga)$ also decreases, but less than $I_{BS}(As)$. This behavior is consistent with the derelaxation of the GaAs(110) surface towards the ideal bulk termination. Assuming for the moment a completely derelaxed surface (i.e., with the ideal bulk termination), new shadowing regions appear because in this case both As and Ga top layers are at the

FIG. 2. TOF spectra for 6 keV Ne[+] acquired at $\phi = -64.7°$, $\theta = 5.5°$ (a), $\theta = 8.3°$ (b) and at three different H$_2$ exposures. Note the strong decrease of $I_{BS}(As)$ with increasing H$_2$ exposure.
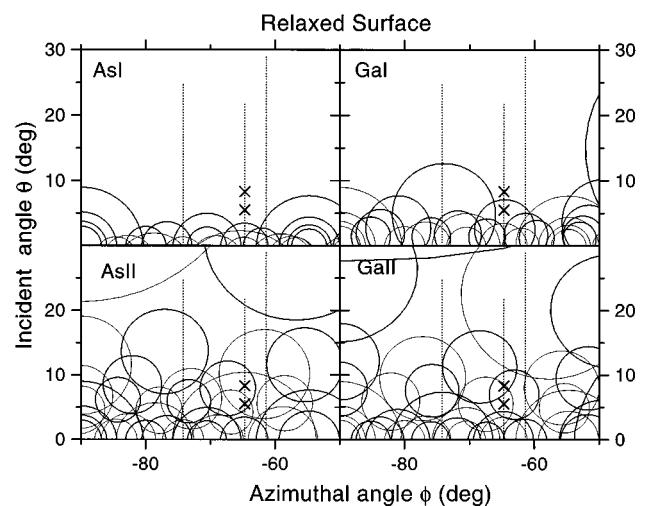
FIG. 3. Shadowing regions calculated for 6 keV Ne[+] backscattering from a relaxed GaAs(110) surface. AsI: first, AsII: second layer of As atoms; GaI: first, GaII: second layer of Ga atoms. The crosses indicate the direction of measurement corresponding to the spectra of Fig. 2. Vertical dashed lines indicate the span of the angular scans shown in Figs. 8–10. Thick and thin lines are shadowing regions produced by As and Ga atoms, respectively.
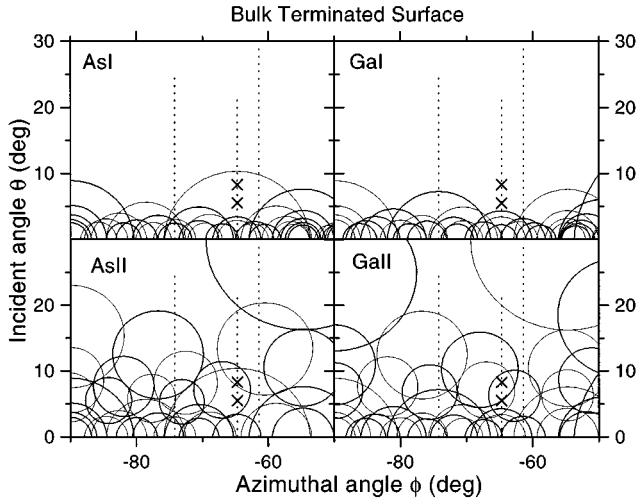
FIG. 4. Similar to Fig. 3 for a bulk terminated surface.

FIG. 5. Shadowing regions for 6 keV Ne$^+$ backscattering from the first layer of As atoms calculated for different Ga, As positions. Thin solid line: shadowing region due to other AsI atoms (independent of the AsI-GaI spacing). Dotted-dashed line: both AsI and GaI atoms in relaxed positions. Dotted line: AsI in bulk and GaI in relaxed positions. Dashed line: AsI in relaxed and GaI in bulk positions. Thick solid line: both atoms in bulk positions. The crosses indicate the directions of measurement for the spectra of Fig. 2.

same height. The new shadowing regions are depicted in Fig. 4. Here we see that the critical angle for focusing onto AsI has moved up to $\theta_c = 10.3°$, which causes the strong decrease observed in $I_{BS}(As)$ at both incidence directions (Fig. 2). For the GaI contribution we see a different effect since, as Ga atoms move up and As atoms down, the critical angle to see the GaI layer decreases to $\theta_c = 4.3°$. In agreement with this, at $\theta = 8.3°$ $I_{BS}(Ga)$ decreases to a steady value [Fig. 2(b)]. On the other hand, at $\theta = 5.5°$ $I_{BS}(Ga)$ does not show a clear enhancement due to the new focusing. We will see in the next section that this absence of focusing can be attributed to ''shadowing'' by the H atoms. We also see in Fig. 4 that the AsII and GaII layers remain shadowed at these incident angles; their contribution appears between $\theta = 15°$ and $20°$ and will be described later.

We have seen that complete derelaxation involving both the As and Ga atoms is in qualitative agreement with the changes observed in the TOF spectra; we can wonder now if it would be possible to describe the experimental data by rasing only the As atoms and leaving the Ga atoms in their relaxed position, or vice versa. The independent effects on the AsI shadowing regions, calculated using the relaxed vertical displacements obtained in paper I, are shown in Fig. 5. The thin line represents the shadowing region due to another AsI atom, which is independent of the AsI-GaI interlayer spacing. This region, together with that due to GaI atoms (dashed-dotted line), forms the total shadowing on the relaxed surface. A vertical shift of the AsI atoms towards their bulk position without moving the GaI atoms changes the shadowing regions as is indicated by the dotted line. In this condition the TOF spectra should be similar to those observed for the clean surface (without the quenching of the AsI contribution), eventually with an increase of the contribution at $\theta = 5.5°$. If only the GaI atoms are moved up (dashed line) leaving the AsI atoms in their relaxed position, the $\theta = 8.3°$ direction should correspond to a focusing direction and should produce an enhancement of $I_{BS}(As)$, instead of the strong decrease observed in the experiment. This indicates that both Ga and As top layers must be at a similar height giving rise to the shadowing region indicated by the
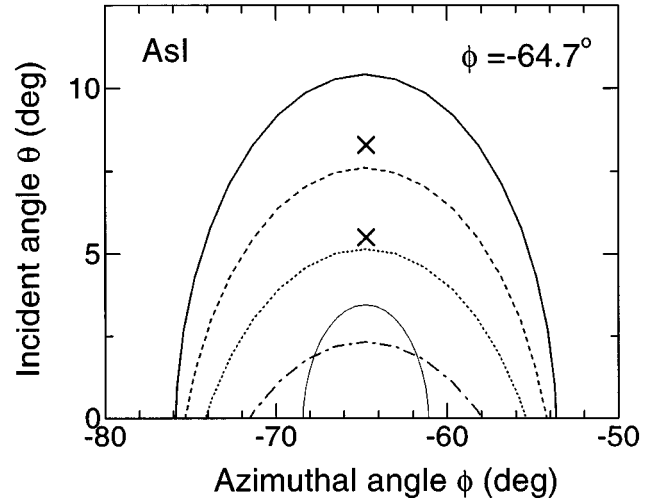
thick line. More precise values for their positions will be derived later from the dependence of $I_{BS}(As)$ and $I_{BS}(Ga)$ with the incident angle.

B. Effect of H on the Ne trajectories

In the precedent discussion we assumed that the changes observed in the TOF spectra are due to derelaxation of the substrate and that the adsorbed hydrogen atoms produce negligible effect on the Ne trajectories. We will now discuss the range of incidence directions in which this assumption is valid. Figure 6(a) shows a trajectory calculation based on the Thomas-Fermi potential with the Molière approximation for 6 keV Ne$^+$ colliding with a H atom. We note that there is a relatively small set of trajectories where the H atom meaningfully scatters the projectile. The focusing effects are not as intense as in the case of Ne scattering from Ga or As
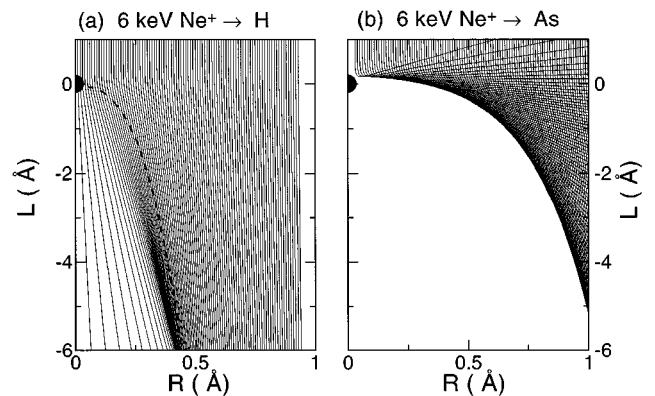

FIG. 6. Trajectory calculations based on a Molière potential for 6 keV Ne$^+$ colliding with a H atom (a) and with an As atom (b). The dashed line in (a) indicates ''H shadow cone'' used to calculate the shadowing regions of Fig. 7.
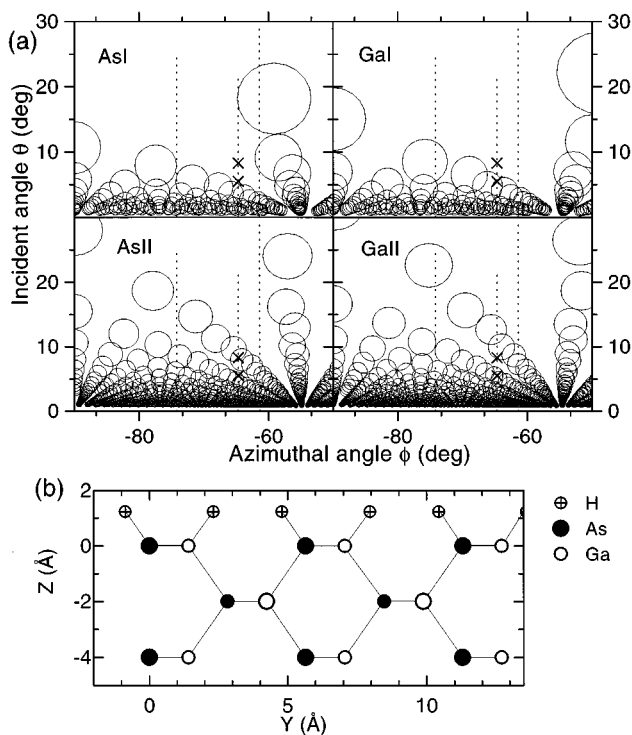
FIG. 7. (a) ''Shadowing regions'' produced by a full ML of H atoms adsorbed along the dangling bonds. Labeling is the same as in Figs. 3 and 4. (b) Side view of the bulk terminated GaAs(110) surface with a full ML of H atoms adsorbed along the dangling bonds.

FIG. 8. (a) Quasisingle backscattering intensity from As atoms ($I_{BS}(As)$) vs incident angle θ measured along $\phi = -64.7°$ for (a) the clean surface and (b) 2000 and 5000 L of H_2. The inset shows a TOF spectrum measured at $(\phi,\theta)=(-64.75°, 8.3°)$. Critical incident angles measured at 70% of the maximum are indicated by vertical segments. The three curves are normalizad with the incident beam intensity.

atoms [shown in Fig. 6(b)], and for small impact parameters the Ne$^+$ penetrates the H ''shadow region.'' With these considerations in mind we construct the equivalent of a H ''shadow cone'' by fitting a curve around the focusing region [dashed line in Fig. 6(a)]. The angular regions where the Ne trajectories are expected to be affected by the H atoms, which we will also call shadow regions, are displayed in Fig. 7(a) for the first and second layer of As and Ga atoms. For the sake of simplicity, and as an extreme case, we have assumed a full ML of H deposited on both As and Ga atoms along the dangling bonds.[16] We have considered a completely derelaxed surface and bond lengths taken from Ref. 16, $d = 1.55$ Å for H-Ga and $d = 1.53$ Å for H-As [Fig. 7(b)]. Even though the shadowing regions are considerably smaller than those corresponding to As or Ga atoms, there are angular regions where the Ne trajectories can be affected by the presence of hydrogen. This is the case for AsI and GaI along $\phi = -64.7°$, at $\theta < 5°$ and $\theta < 7°$, respectively. Outside these shadowing regions, the changes in the TOF spectra should reflect the changes in the substrate structure due to H adsorption.

C. Dependence of the TOF spectra on the incident angle

1. $\phi = -64.7°$

In order to get quantitative information about the interlayer spacing after exposure to H_2 one might be tempted to measure the backscattered intensity along $\phi = -35°$, corresponding to the bond direction, Fig. 1(c). This is not a good choice because, along this direction, the second layer of the
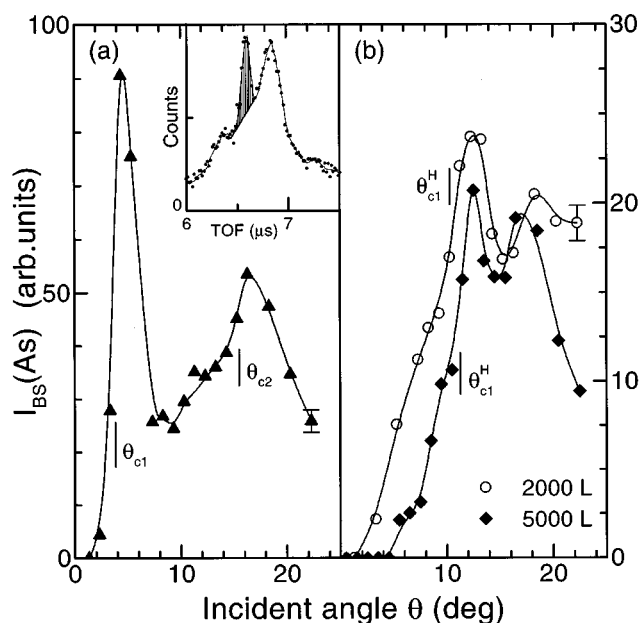
derelaxed surface contributes with strong focusing at a similar incident angle to the first layer, making the analysis much more difficult. Along $\phi = -64.7°$ and at low incident angles the derelaxed GaI atoms shadow the AsI atoms and the contributions from the first and second layers appear well separated (Fig. 4); both effects combine to make this azimuthal orientation very sensitive to the AsI-GaI spacing.

The quantitative analysis of the backscattered intensity requires the separation of quasisingle and multiple contributions. Following paper I, we have computed the quasisingle backscattering intensity from As as indicated in the inset of Fig. 8(a). This method minimizes uncertainties owing to multiple-scattering contributions from Ga atoms (paper I). $I_{BS}(As)$ measured for the clean surface along $\phi = -64.7°$ is shown in Fig. 8(a) as a function of the incident angle. The first critical angle θ_{c1} corresponds to focusing on an AsI atom by another AsI atom located at 18.7 Å. The second critical angle θ_{c2} is due to focusing onto AsII atoms which become visible to the beam only between $\theta = 15°$ and $20°$; these features are clearly seen in the shadowing regions of Fig. 3.

$I_{BS}(As)$ measured along $\phi = -64.7°$ as a function of the incident angle after exposing the surface to two H_2 doses is shown in Fig. 8(b). For the hydrogenated surfaces the first layer focusing is less intense and has shifted to $\theta_{c1}^H = 10.3°$ at 2000 L and to $11.3°$ at 5000 L; the contribution from the second layer appears at approximately the same angle and is considerably less intense (note the different vertical scales). Since for $\theta > 5°$ $I_{BS}(As)$ is not affected by the H atoms (Fig. 7), the new first layer critical angles can be related to a focusing of the Ne trajectories onto AsI atoms, produced by derelaxed GaI atoms (Fig. 4). From the experimental critical

angles $\theta_{c1}^H = (10.3 \pm 1)°$ and $\theta_{c1}^H = (11.3 \pm 1)°$ and following the procedures of paper I, we infer values for the AsI-GaI new spacings of $\Delta Z = (0.0 \pm 0.08)$ Å and $\Delta Z = (-0.08 \pm 0.08)$ Å for the surface exposed to 2000 L and 5000 L, respectively. Assuming that ΔY [Fig. 1(a)] is the same as in the bulk terminated surface we have obtained buckling angles $\omega = (0 \pm 3)°$ for a 2000 L exposure and $\omega = (-3 \pm 3)°$ for 5000 L (the errors mainly come from the uncertainty in the background subtraction).

The decrease in the intensity of the first layer focusing is attributed to the decrease in the interatomic distance between the atoms participating in the focusing. For the clean surface this distance is large, 18.7 Å (corresponding to two AsI atoms) and the complete focusing is over in $\sim 5°$. In the hydrogenate surface the distance between an AsI and a GaI in a derelaxed position is 4.7 Å and therefore the focusing is less intense (thermal vibrations are more important) and spans over a wider angular range. The decrease of the second layer focusing is also consistent with the derelaxation process, the gap between the two shadowing regions (between 15° and 20°) becomes smaller (Figs. 3 and 4) making weaker the single-backscattering contribution from AsII.

2. $\phi = -74.2°$

At the azimuthal direction discussed above we have taken advantage of the fact that for the derelaxed surface the Ga atoms shadow the As atoms. At $\phi = -74.2°$ the situation is reversed, As atoms shadow the Ga atoms [see Fig. 1(a)]; the behavior of $I_{BS}(Ga)$ with θ should also be sensitive to the AsI-GaI spacing. The corresponding $I_{BS}(Ga)$ vs θ curves for the clean and for the surface exposed to 1000 L are shown in Fig. 9. For the clean surface we observe a single peak with a critical angle $\theta_c = 13°$. We see from the shadowing regions of Fig. 3 that the second layer of Ga atoms contributes to $I_{BS}(Ga)$ at an incident angle close to that of the first layer. The peak observed in Fig. 9 is the sum of the contribution from each layer. After H adsorption the dependence of $I_{BS}(Ga)$ vs θ changes. Between $\theta = 7°$ and $12°$ $I_{BS}(Ga)$ increases while the contribution above $\theta = 12°$ shifts to larger incident angles. The shadowing regions calculated for the derelaxed surface (Fig. 4) indicate that the focusing on GaI atoms should occur at a smaller incident angle (around $\theta = 7°$) and the contribution from GaII should move towards larger incident angles ($\theta = 18.5°$). The fact that the intensity around $\theta \sim 15°$ remains high suggest that at 1000 L a fraction of the surface remains relaxed.

Contrary to the previous case, at this azimuthal direction the H atoms can affect the Ne trajectories for $\theta < 11°$, softening the focusing effect on the Ga atoms (Fig. 7). This can be the reason why the GaI focusing seen at $\theta_{c1}^H = 7.4°$ is very weak. In correspondence with this, $I_{BS}(Ga)$ shows a rise at $\theta_{c2}^H = 10.6°$, which can be assigned to focusing by the H atoms [Fig. 7(a), GaI].

If we neglect the effect of hydrogen and consider the critical angle observed at $\theta_c^H = 7.4°$ as representative of the focusing on the GaI atoms by AsI atoms, we obtain an AsI-GaI spacing of $\Delta Z = (0.0 \pm 0.1)$ Å, which confirms the value obtained at $\phi = -64.7°$ for the intermediate dose.
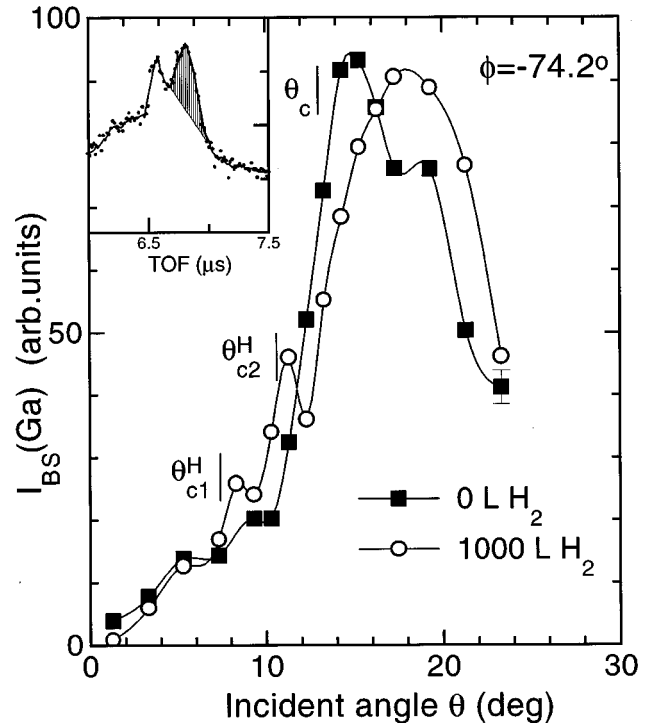
FIG. 9. Quasisingle backscattering intensity from Ga atoms vs incident angle along $\phi = -74.2°$. Solid symbols: clean surface, open symbols: surface exposed to 1000 L of H_2. The inset shows a TOF spectrum measured at $(\phi, \theta) = (-74.2°, 16.3°)$.

3. $\phi = -61.4°$

At $\phi = -61.4°$ $I_{BS}(Ga)$ presents an interesting effect coming from the contribution of GaII which, for large incident angles should not be affected by the presence of H. Figure 10 shows $I_{BS}(Ga)$ for the clean surface and for a 1000 L exposure. $I_{BS}(Ga)$ for the clean surface presents one critical angle at $\theta = 5.8°$ due to focusing on a first layer Ga atom. The second layer is inside a big shadowing region (Fig. 3) and does not contribute, i.e., $I_{BS}(Ga)$ goes down at larger θ and then remains constant. The changes observed after H adsorption are consistent with the derelaxation process. The critical angle for the first layer contribution should move down from 6° to about 4° (Fig. 3 and 4). At this θ the H atoms may alter the Ne trajectories, reducing the focusing effect of the AsI atoms. We also see in these figures that if the surface becomes derelaxed, a contribution from GaII, not present in the clean surface, should appear between $\theta = 10°$ and $\theta = 18°$. In agreement with this model we can identify in Fig. 10 a first rise of $I_{BS}(Ga)$ (around 4.3°) and a larger intensity between $\theta = 12°$ and 19°. $I_{BS}(Ga)$ reduces to the first layer value at $\theta > 20°$ as in the clean case, when the second layer contribution disappears because of the large shadowing region produced by a first layer Ga atom.

We note that this effect is the reverse of the effect observed at $\phi = -64.7°$, where the second layer contribution decreases due to the surface derelaxation. From the critical angle at $\theta_{c3}^H = 15.3°$ (Fig. 10) it is possible to obtain the value of the spacing between the GaI and GaII layers; we did not use the rise $\sim 8°$ because it might be affected by a contribution from surface regions that at a 1000 L dose remain re-

FIG. 10. Similar to Fig. 9 along $\phi = -61.4°$.

FIG. 11. Quasisingle backscattering intensity from As atoms vs H_2 exposure along $(\phi, \theta) = (-64.7°, 6.3°)$. The inset is an expanded view of the low exposure region.

laxed (as clean regions). Following the procedure used for the AsI-GaI spacing, we have obtained a GaI-GaII spacing $\Delta Z_{1,2}^{Ga} = (1.8 \pm 0.1)$ Å.

D. Dependence of TOF spectra on the H_2 exposure

In order to gain some insight about the dependence of the derelaxation process on exposure we have taken TOF spectra at a fixed incidence direction $(\phi, \theta) = (-64.7°, 6.3°)$, as a function of the H_2 dose. At this incidence direction some AsI focusing is still present [Fig. 8(a)], while the AsII layer do not contribute to $I_{BS}(As)$ (Figs. 3 and 4) and the H atoms do not affect the Ne trajectories (Fig. 7). As we have discussed above, the pairs of consecutive GaI and AsI 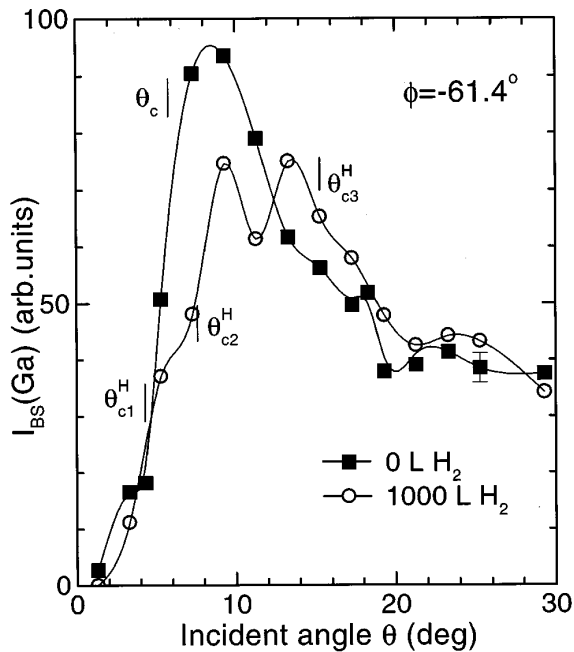atoms that are along the projectile direction and remain relaxed contribute to $I_{BS}(As)$, while those that have undergone derelaxation do not contribute. The decrease of $I_{BS}(As)$ with the H_2 exposure should then be directly related to the fraction of the surface that have undergone derelaxation.

$I_{BS}(As)$ is shown in Fig. 11 as a function of the H_2 exposure; the low exposure region is expanded in the inset. $I_{BS}(As)$ presents a monotonous decrease up to 5000 L, i.e., at this exposure the process reach a steady regime. An interesting feature observed in this figure is the very fast decrease of $I_{BS}(As)$ at the beginning of the exposure, at 400 L it has already decreased to one half of its initial value.

IV. SUMMARY AND CONCLUSIONS

The behavior of the Ne quasisingle backscattered intensity coming from the first two As and Ga layers is consistent with a process of derelaxation towards the ideal surface termination. Comparison with simple calculations of the shadowing regions corresponding to relaxed and bulk terminated surface allowed us to interpret details such as the appearance and decrease of some Ga and As second layer contributions,
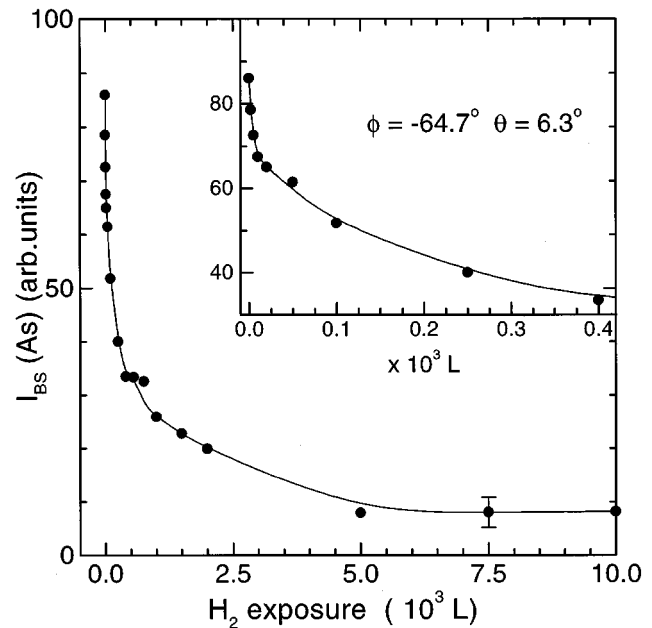
respectively. The effect that the adsorbed H atoms have on the Ne trajectories was discussed by assuming an adsorption geometry along the dangling bonds.[16] Although we do not have a clear proof of the adsorption geometry, the relatively low intensity of the first layer focusings observed along $\phi = -74.2°$ and $\phi = -61.4°$, and the rise of $I_{BS}(Ga)$ seen at $(\phi, \theta) = (-74.2°, 10.6°)$ is consistent with hydrogen atoms adsorbed along the dangling bonds. The hydrogen shadowing effect was minimized by choosing measurement directions such that the focusing effects of interest (due to As or Ga atoms) were far from the shadowing regions produced by H atoms.

From the measurement of $I_{BS}(As)$ as a function of the incident angle we have determined that for exposures of 1000 L and 2000 L the AsI-GaI splitting corresponding to the derelaxed surface is already reduced to $\Delta Z = (0.0 \pm 0.08)$ Å, as is expected for the bulk terminated surface. At these exposures there is a fraction of the surface that remains relaxed. On the other hand, at 5000 L, when most of the surface has been derelaxed, our data is consistent with a small counter-relaxation, with a buckling angle $\omega = (-3 \pm 3)°$. This value corresponds to a AsI-GaI splitting of only $\Delta Z = (-0.08 \pm 0.08)$ Å and is within the limit of sensitivity of the technique. Comparison of the critical angles with calculated shadowing regions allowed us to determine the distance between first (derelaxed) and the second layer. The value obtained is $\Delta Z_{1,2} = (1.8 \pm 0.1)$ Å, which is smaller than the one corresponding to the relaxed bulk atomic structure, $\Delta Z_{1,2} = 2.0$ Å.

The vertical displacements obtained in this work, are similar to those proposed by other authors using diffraction techniques[14,15] (see Table I). The experimental values present a dependence on the H_2 dose. For higher exposures, 5000 L in our case, a counter-relaxation is observed in agreement with calculations for a full ML of adsorbed H atoms

TABLE I. Vertical spacing between AsI and GaI (ΔZ) and buckling angle ω obtained with different H_2 exposures and methods.

$\Delta Z(\text{Å})$	ω	Coverage (ML)	H_2 exposure	Method
-0.115	-5 ± 1	0.8	4500 L	GIXD [a]
0.15	6 ± 1.5	0.25	100 L	PD [b]
0.0 ± 0.08	0 ± 3		1000 L	TOF-ISS [c]
-0.08 ± 0.08	-3 ± 3		5000 L	TOF-ISS [d]
	-5	1		Total Energy [e]
-0.076	-3.1	1		total energy [f]
-0.949	-7.1	1		total energy [g]
	6	0.25		molecular dynamics [h]

[a]Reference 14.   [e]Reference 16.
[b]Reference 15.   [f]Reference 17.
[c]This work.   [g]Reference 18.
[d]This work.   [h]Reference 19.

(Table I). In the determination of the vertical displacement with TOF-ISS, it is not necessary to relate the H_2 exposure to a specific H coverage. This is due to the fact that there are some incident directions where the contribution from relaxed and derelaxed fractions of the surface appear separated. Contrary to this, in GIXD experiments[14] the structural analysis is strongly dependent on the assumed H coverage.

The dependence of $I_{BS}(As)$ (representative of the fraction of the surface remaining relaxed) on H_2 is far from being linear. $I_{BS}(As)$ decreases very fast up to 400 L, at higher exposures the rate of derelaxation becomes slower and finally at 5000 L $I_{BS}(As)$ reaches a steady stage corresponding to a small fraction of the surface remaining relaxed (~ 10 %). This suggests that at 5000 L the H coverage is around 1 ML. A similar dependence was observed before[13] from the analysis of the variation of the LEED spot intensity and of photoemission yields with the H_2 dose. The behavior of $I_{BS}(As)$ with the H exposure, together with the dependence of $I_{BS}(As)$ and $I_{BS}(Ga)$ on the incidence direction, indicates that a relatively large fraction of the surface still remains relaxed at intermediate exposures (between 1000 and 2000 L). At present we cannot relate the behavior of $I_{BS}(As)$ to a change in the H adsorption rate or with a change in the fraction of the surface derelaxed by each H atom, i.e., to the local or nonlocal character of the derelaxation process at low exposures. This information might be obtained from a simultaneous measurement of $I_{BS}(As)$ and of the intensity of H atoms recoiled at forward angles as a function of the exposure, an experiment that we plan to perform in the near future.

[1] C. B. Duke, S. L. Richardson, A. Paton and A. Kahn, Surf. Sci. **127**, L135 (1983).

[2] S. Y. Tong, W. N. Mei and G. Xu, J. Vac. Sci. Technol. B **2**, 393 (1984).

[3] L. Smit, T. E. Derry, and J. F. Van Der Veen, Surf. Sci. **150**, 245 (1985).

[4] R. M. Feenstra, J. A. Stroscio, J. Tersoff, and A. P. Fein, Phys. Rev. Lett. **58**, 1192 (1987).

[5] J.E. Gayone, R.G. Pregliasco, G.R. Gómez, E.A. Sánchez, and O. Grizzi, Phys. Rev. B **56**, 4186 (1997).

[6] C. Mailhiot, C. B. Duke, and D. J. Chadi, Surf. Sci. **149**, 366 (1985).

[7] J. L. Alves, J. Hebesntreit, and M. Scheffler, Phys. Rev. B **44**, 6188 (1991).

[8] H. Lüth and R. Matz, Phys. Rev. Lett. **46**, 1652 (1981).

[9] U. del Pennino, C. Mariani, A. Amoddeo, F. Proix, and C. A. Sébenne, Physica B **170**, 487 (1991).

[10] F. Antonangeli, C. Calandra, E. Colavita, S. Nannarone, C. Rinaldi, and L. Sorba, Phys. Rev. B **29**, 8 (1984).

[11] A. Santoni, L. Sorba, D. K. Shuh, L. J. Terminello, A. Franciosi, and S. Nannarone, Surf. Sci. **269/270**, 893 (1992).

[12] A. Plesanovas, A. Castellani Tarabini, I. Abbati, S. Kaciulis, G. Paocelli, L. Pasquali, A. Ruocco, and S. Nannarone, Surf. Sci. **307-309**, 890 (1994).

[13] O. M'Hamedi, F. Proix, and C. Sébenne, Semicond. Sci. Technol. **2**, 418 (1987).

[14] A. Ruocco, S. Nannarone, M. Sauvage-Simkin, N. Jedrecy, R. Pinchaux, and A. Waldhauer, Surf. Sci. **307-309**, 662 (1994).

[15] A. Ruocco, M. Biagini, A. di Bona, N. Gambacorti, S. Valeri, and S. Nannarone, Phys. Rev. B **51**, 2399 (1995).

[16] C. M. Bertoni, M. Buongiorno Nardelli, F. Bernardini, F. Finoc-

chi, and E. Molinari, Europhys. Lett. **13**, 653 (1990).

[17] A. F. Wright, C. Y. Fong, and I. P. Batra, Surf. Sci. **244**, 51 (1991).

[18] J. Fritsch, A. Eckert, P. Pavone, and U. Scrö, J. Phys. Condens. Matter **13**, 653 (1990).

[19] R. Di Felice, A. I. Shkrebtii, F. Finocchi, C. M. Bertoni, and G. Onida, J. Electron Spectrosc. Relat. Phenom. **64/65**, 697 (1993).

[20] O. S. Oen, Surf. Sci. **131**, L470 (1983).

[21] R. G. Pregliasco, J. E. Gayone, E. A. Sánchez, and O. Grizzi (unpublished).